



Semnan University



## Investigating of Fluid Flow and Heat Transfer MWCNT-Fe<sub>3</sub>O<sub>4</sub> Hybrid Nanofluid Inside Integrated Solar Collector Storage

Rasul Mohebbi <sup>a,\*</sup>

<sup>a</sup> School of Engineering, Damghan University, Damghan, Iran; P.O. Box: 36716411671

\*Corresponding author: [rasul\\_mohebbi@du.ac.ir](mailto:rasul_mohebbi@du.ac.ir)

Received: 2024-08-06 Revised: 2025-04-05 Accepted: 2025-05-12

### Abstract

The need for clean energy in today's world is increasing day by day due to the limited nature of fossil resources. Solar energy can be utilized in various domestic, agricultural, and industrial applications. Integrated solar storage collectors are extensively used for generating heat by absorbing solar energy and converting it into thermal energy. Therefore, there is a significant need to design and produce these collectors to achieve the highest performance and efficiency. In this research, considering a type of integrated solar storage collector and using the hybrid nanofluid MWCNT-Fe<sub>3</sub>O<sub>4</sub>, its effect at different Rayleigh numbers (103-106) and various nanofluid percentages (0-0.003) has been investigated. Velocity and temperature contours and streamlines in different positions of the hot absorber inside the collector have been examined. The local and average Nusselt numbers have also been studied. The results indicate an increase in heat transfer at the Rayleigh number and a high percentage of nanofluid. Additionally, the optimal position for placing the hot absorber is at the far right end of the collector. The results of this research are published for the first time and can be used for designing solar collectors.

### Keywords

Nanofluid, Integrated Solar Collector Storage, Fluid Flow, Nusselt number.

### 1. Introduction

The rapid development of modern societies, accompanied by significant advances in technology across various fields of medical and engineering sciences, has led to an increasing demand for affordable, renewable, and clean energy sources. Changes in lifestyle and rising expectations for improved quality of life have motivated scientists to explore diverse methods of energy generation and to enhance the efficiency of energy systems. Fossil fuels, which currently constitute the primary source of energy, face two major challenges: global warming and environmental pollution, as well as limited availability due to their non-renewable nature [1].

At present, the main renewable energy sources include solar, wind, hydropower, tidal, and geothermal energy. Among these, solar energy offers outstanding advantages owing to its cleanliness, safety, and abundance. Unlike wind power plants, which are often located in remote areas with limited access to end users, solar energy systems can be installed near consumption centers. This feature reduces the need for long-distance transmission lines and alleviates pressure on energy transmission infrastructures [2].

Space heating in buildings has always been a critical issue in countries with cold climates. Solar-based space heating is not only environmentally friendly but also requires lower maintenance and operational costs compared to conventional heating methods. One practical application of renewable energy is low-temperature water heating, which is typically achieved using thermosyphon solar collectors and integrated collector-storage (ICS) units. The design and construction of these solar water heaters depend on the operational requirements of each application and the climatic conditions of the installation site. Generally, these systems are suitable for small-scale applications, such as domestic water heaters with capacities of 100–200 liters per day. Ensuring reliability, high efficiency, and ease of maintenance is essential for their effective contribution to sustainable energy supply [3].

The most important aspect in the utilization of these storage systems is the design of integrated collector-storage (ICS) units that are simpler, more cost-effective, more durable, and capable of achieving maximum efficiency and optimal performance. Numerous researchers have investigated this topic. Reddy et al. [4] developed a thermal flux distribution model for a solar concentrator system using a phased-focus dish with an area of 20 m<sup>2</sup>. They reported an average heat transfer efficiency of 74% for a parabolic dish collector with a modified cavity at a flow rate of 250 L/h. Soltani et al. [5] established a relationship between the geometric and operational parameters of a cylindrical cavity receiver, considering natural convection over a downward-heated flat surface. Si-Kwan et al. [6] investigated the optical and thermodynamic

performance of a spherical cavity receiver. Their results indicated that the optical efficiency of the spherical cavity receiver reached 88.9%, which is slightly higher than that of cylindrical, conical, and truncated conical cavity receivers.

Numerous studies have focused on enhancing heat transfer in various geometries and solar collectors [7]. The use of different nanofluids, in combination with conventional enhancement techniques, has attracted considerable attention. Tajik et al. [8] experimentally investigated the rheological properties of non-Newtonian nanofluids, employing  $\text{Al}_2\text{O}_3$ ,  $\text{TiO}_2$ , and  $\text{CuO}$  nanoparticles as working fluids.

Waghel et al. [9] experimentally studied the effects of using a silver/water nanofluid and twisted tape inserts in the absorber tube of a parabolic trough solar collector. Their results showed that the Nusselt number in the absorber tube equipped with twisted tape was 1.25 to 2.1 times higher than that of a plain tube. Chang et al. [10] employed a straight thin rod inside the absorber tube and used molten salt as the working fluid. Their findings demonstrated that increasing the rod diameter enhanced the Nusselt number by a factor ranging from 1.1 to 7.42 compared to a conventional absorber tube.

Due to the lack of available information on the performance of integrated collector–storage systems and the effect of nanofluids on their efficiency, the present study, for the first time, investigates a concentrated solar collector containing a hybrid nanofluid composed of multi-walled carbon nanotubes and iron oxide nanoparticles. The displacement of the absorber is examined to identify the optimal collector design under various Rayleigh numbers and nanoparticle volume fractions. The findings of this study are of significant importance. The geometry under investigation has been selected based on previous studies and common practical applications of integrated solar collector–storage systems, ensuring that the present research offers greater practical relevance and applicability

## 2. Geometry under Consideration

In this study, two-dimensional fluid flow and heat transfer within an integrated collector–storage (ICS) solar collector, as illustrated in Figure 1, are investigated. In the presented geometry, the characteristic length  $L$  is equal to 1 m, and the corresponding radii are defined as follows:

$$R_1=0.27 \text{ m}$$

$$R_2=0.54 \text{ m}$$

$$R_3=0.85 \text{ m}$$

The OBC section is composed of an elliptical shape. The working fluid employed in this study is a hybrid nanofluid consisting of multi-walled carbon nanotubes and iron oxide nanoparticles (MWCNT- $\text{Fe}_3\text{O}_4$ ) dispersed in water. The OC wall is maintained at a cold temperature of  $T_c=0 \text{ K}$ , while the temperature of the heated obstacle is assumed to be  $T_h=1 \text{ K}$ . All remaining walls are considered adiabatic. Density variations are modeled using the Boussinesq approximation, and the flow regime is assumed to be laminar. Gravitational acceleration is included to induce buoyancy effects resulting from density differences. It is assumed that no slip occurs between the base fluid and the nanoparticles, and thermal equilibrium between the water and nanoparticles is maintained. The rate of heat transfer inside the cavity is evaluated over a wide range of Rayleigh numbers by calculating the Nusselt number along the heated walls.

In this study, the heated obstacle is positioned at three different locations:

- the far left side,
- the central position, and
- the far right side of the cavity.

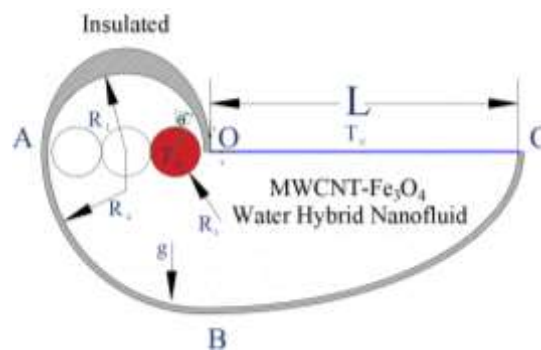


Figure 1. Geometry under consideration

## 3. Thermophysical Properties of the Nanofluid

The density, specific heat capacity, thermal diffusivity, volumetric thermal expansion coefficient, and Prandtl number of the nanofluid are respectively defined as follows [16,17]:

$$\rho_{nf} = (1 - \phi)\rho_f + \phi\rho_p \quad (1)$$

$$(\rho c_p)_{nf} = (1 - \phi)(\rho c_p)_f + \phi(\rho c_p)_p \quad (2)$$

$$(\rho\beta)_{nf} = (1 - \phi)(\rho\beta)_f + \phi(\rho\beta)_p \quad (3)$$

$$\alpha_{nf} = \frac{k_{nf}}{(\rho c_p)_{nf}} \quad (4)$$

$$\text{Pr}_{nf} = \frac{(\mu c_p)_{nf}}{k_{nf}} \quad (5)$$

where  $\phi$  denotes the nanoparticle volume fraction, and the subscripts  $f$ ,  $nf$ , and  $p$  represent the base fluid, nanofluid, and nanoparticles, respectively.

#### 4. Validation

To demonstrate the reliability and accuracy of the numerical method, the present results are compared with data available in the literature. To further verify the accuracy of the numerical code against previously published results, the streamlines and isotherms for natural convection inside a square cavity containing a heated obstacle at a Rayleigh number of  $10^3$  are compared with the simulation results reported by Chen et al. [11]. The close agreement between the two sets of results demonstrates the high accuracy and reliability of the numerical code employed in the present study.

#### 5. Results and Discussion

Figure 2 illustrates the streamlines for pure water ( $\phi=0$ ) when the heat source is located at position (a), i.e., at the far left side of the cavity, for different Rayleigh numbers. Initially, due to the steady-state flow regime, the flow structure inside the cavity consists of a single dominant vortex. At  $\text{Ra}=10^3$ , the vortex exhibits an approximately elliptical shape. As the Rayleigh number increases to  $10^6$ , the streamline patterns at different layers undergo noticeable changes, and the streamlines tend to conform more closely to the overall cavity geometry. This behavior is attributed to the intensified convective motion resulting from the increase in the Rayleigh number. At the maximum Rayleigh number considered, a large horizontally oriented elliptical vortex, slightly shifted toward the left side of the cavity, is formed.

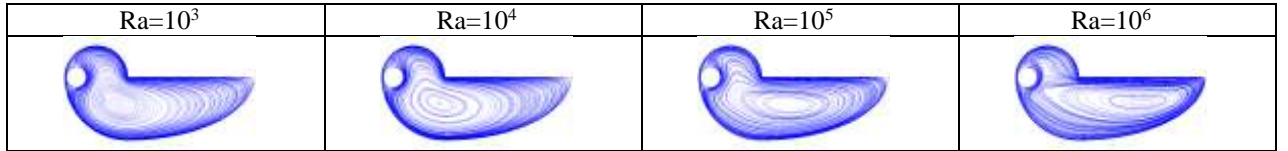
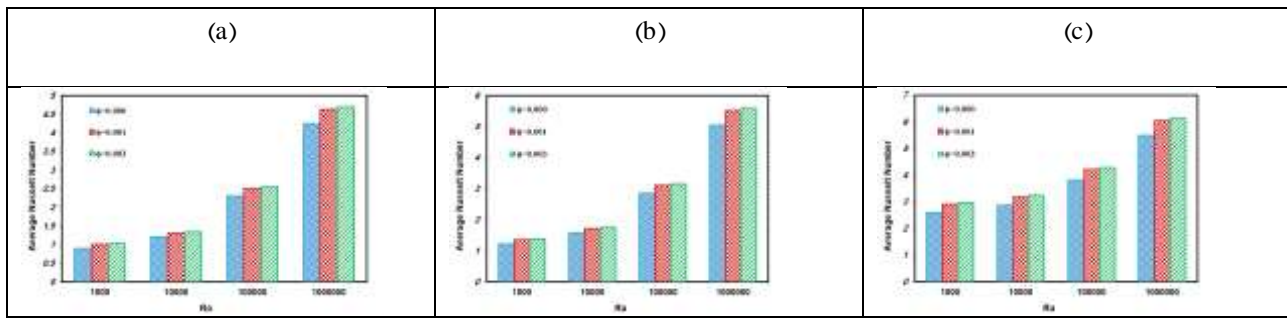


Figure 2. Streamlines for position (a) at different Rayleigh numbers for  $\phi=0.00$ .

Figure 3 presents the average Nusselt number values for different nanoparticle volume fractions ( $\phi$ ) and Rayleigh numbers ( $\text{Ra}$ ) for various positions of the heated obstacle within the cavity. By comparing different configurations, it is observed that as the heat source moves from the left side toward the right side of the cavity, the average Nusselt number increases for all Rayleigh numbers. This behavior can be attributed to the fact that when the heat source is located closer to the right side of the cavity, it becomes nearer to the cold wall, which significantly enhances the heat transfer characteristics. According to Figure 4, the average Nusselt number ( $\text{Nu}_{ave}$ ) increases with increasing Rayleigh number and nanoparticle volume fraction, regardless of the heat source position. As can be seen, increasing the nanoparticle volume fraction directly leads to an increase in the Nusselt number and an enhancement of the heat transfer rate. This improvement is mainly due to the increased thermal conductivity of the nanofluid resulting from the presence of nanoparticles. This effect is particularly important in the design of solar collectors, as employing nanofluids with higher volume fractions can lead to improved system efficiency by enhancing thermal energy absorption and transfer. Therefore, selecting an optimal nanoparticle volume fraction is of great importance for improving the performance of solar collectors.



**Figure 3. Variation of the average Nusselt number versus Rayleigh number for the heated obstacle located at different positions: (a) position a, (b) position b, and (c) position c.**

## 6. Conclusions

In this study, natural convection of a nanofluid inside an integrated solar collector–storage system containing a heated obstacle was investigated. The effects of the Rayleigh number (Ra), nanoparticle volume fraction, and heat source location on the convection process were analyzed. The results indicate that the average Nusselt number increases with increasing Rayleigh number and nanoparticle volume fraction. Moreover, relocating the heat source from the left side to the right side of the cavity leads to a noticeable improvement in heat transfer performance. The optimum heat transfer condition was observed at  $Ra=10^6$  and  $\phi=0.003$ , with the heat source located at the far right side of the cavity. The findings further demonstrate that the simultaneous increase in nanoparticle volume fraction and Rayleigh number results in a substantial enhancement of heat transfer. In this regime, the presence of high-thermal-conductivity nanoparticles and strong convective flow act synergistically to provide optimal heat transfer conditions. Therefore, an optimal solar collector design can be achieved through a combination of using nanofluids with higher volume fractions and adjusting thermal operating conditions to attain higher Rayleigh numbers. These results offer valuable insights for the design and development of high-performance solar collectors

## 7. References

- [1] Atems, B., and C. Hotaling. "The effect of renewable and nonrenewable electricity generation on economic growth." *Energy Policy* 112, (2018): 111–118.
- [2] Vahidhosseini, Seyed Mohammad, Saman Rashidi, Shu-Han Hsu, Wei-Mon Yan, and Abbas Rashidi. "Integration of solar thermal collectors and heat pumps with thermal energy storage systems for building energy demand reduction: A comprehensive review." *Journal of Energy Storage* 95, (2024): 112568.
- [3] Tripanagnostopoulos, Y., and P. Yianoulis. "Integrated collector-storage systems with suppressed thermal losses." *Solar Energy* 48, no. 1 (1992): 31-43.
- [4] Reddy, K.S., S.K. Natarajan, and G. Veershetty. "Experimental performance investigation of modified cavity receiver with fuzzy focal solar dish concentrator." *Renew Energy*, no. 74 (2015): 148-57.
- [5] Soltani, S., M. Bonyadi, and A.V. Madadi. "A novel optical-thermal modeling of a parabolic dish collector with a helically baffled cylindrical cavity receiver." *Energy*, no. 168 (2019): 88-98.
- [6] Si-Quan, Z., L. Xin-Feng, D. Liu, and M. Qing-Song. "A numerical study on optical and thermodynamic characteristics of a spherical cavity receiver." *Appl Therm Eng*, no. 149 (2019): 11–21.
- [7] Mohebbi, R., Y. Ma, and P. Soleymani. "Investigating the Impact of Sinusoidal Walls on Fluid Flow and Heat Transfer Performance of C-Shaped Cavity." *Iran J Sci Technol Trans Mech Eng* (2024). <https://doi.org/10.1007/s40997-024-00781-y>
- [8] Tajik Jamal-Abad, M., M. Dehghan, S. Saedodin, M.S. Valipour, A. Zamzamin. "An experimental investigation of rheological characteristics of non-Newtonian nanofluids." *J Heat Mass Transf Res* 1, no. 1 (2014): 17–23.
- [9] Waghole, D.R., R. Warkhedkar, and R. Shrivastva. "Experimental investigations on heat transfer and friction factor of silver nanofluid in absorber/receiver of parabolic trough collector with twisted tape inserts." *Energy Procedia*, no. 45 (2014): 558-67.
- [10] Chang, C., A. Sciacovelli, Z. Wu, X. Li, Y. Li, M. Zhao, et al. "Enhanced heat transfer in a parabolic trough solar receiver by inserting rods and using molten salt as heat transfer fluid." *Appl Energy*, no. 220 (2018): 337-50.
- [11] Chen, Z., C. Shu, L.M. Yang, X. Zhao, and N.Y. Liu. Immersed boundary–simplified thermal lattice Boltzmann method for incompressible thermal flows Editor’s Pick, *Phys. Fluids* 32, 013605 (2020).